We are IntechOpen, the world's leading publisher of Open Access books Built by scientists, for scientists

4,800
Open access books available

122,000
International authors and editors

135M
Downloads

Our authors are among the

154
Countries delivered to

TOP 1%
most cited scientists

12.2%
Contributors from top 500 universities

CLARIVATE ANALYTICS

BOOK CITATION INDEX

INDEXED

WEB OF SCIENCE™

Selection of our books indexed in the Book Citation Index
in Web of Science™ Core Collection (BKCI)

Interested in publishing with us?
Contact book.department@intechopen.com

The Gas Environmental Chamber as a Powerful Tool to Study Structural Changes of Living Muscle Thick Filaments Coupled with ATP Hydrolysis

Haruo Sugi, Hiroki Minoda, Takuya Miyakawa,
Suguru Tanokura, Shigeru Chaen and Takakazu Kobayashi

Additional information is available at the end of the chapter

1. Introduction

The gas environmental chamber (or the hydration chamber) has been developed to observe chemical reactions in water solutions under high magnifications with an electron microscope (for an extensive review, see Buttler & Hale, 1981). The gas environmental chamber (EC) has been widely used for *in situ* observation of inorganic substances in the field of materials science. Fig.1 shows two different types of the EC. One is film-sealed EC, which is insulated from high vacuum of electron microscope with sealing film at is upper and lower windows to pass electron beam (Fig.1A). Water vapor (water gas) is constantly circulated through the EC to keep the specimen in hydrated state. The other is aperture-limited EC, which has apertures to pass electron beam without any sealing film. Water gas is constantly injected into the EC, and sucked out of the EC to keep the specimen in hydrated state (Fig.1B).

In the research field of medical and biological sciences, it was a dream of investigators to observe living microorganisms moving under an electron microscope with high magnifications. In order to realize this dream, a number of attempts have hitherto been made to observe living microorganisms by means of the EC attached to an electron microscope. Such attempts have been, however, found to be unsuccessful because the function of living microorganisms are readily impaired by electron beam irradiation. On the other hand, the function of biological macromolecules, such as proteins and lipids, are expected to be much more resistant against electron beam irradiation. The experiments to be described in this chapter were started to ascertain whether the EC was useful in studying dynamic structural

changes of biological macromolecules related to their function. After many considerations, we decided to study molecular mechanism of muscle contraction using the EC, which was designed and constructed to be suitable for physiological experiments to investigate dynamic structural changes of hydrated muscle myosin filaments coupled with ATP hydrolysis.
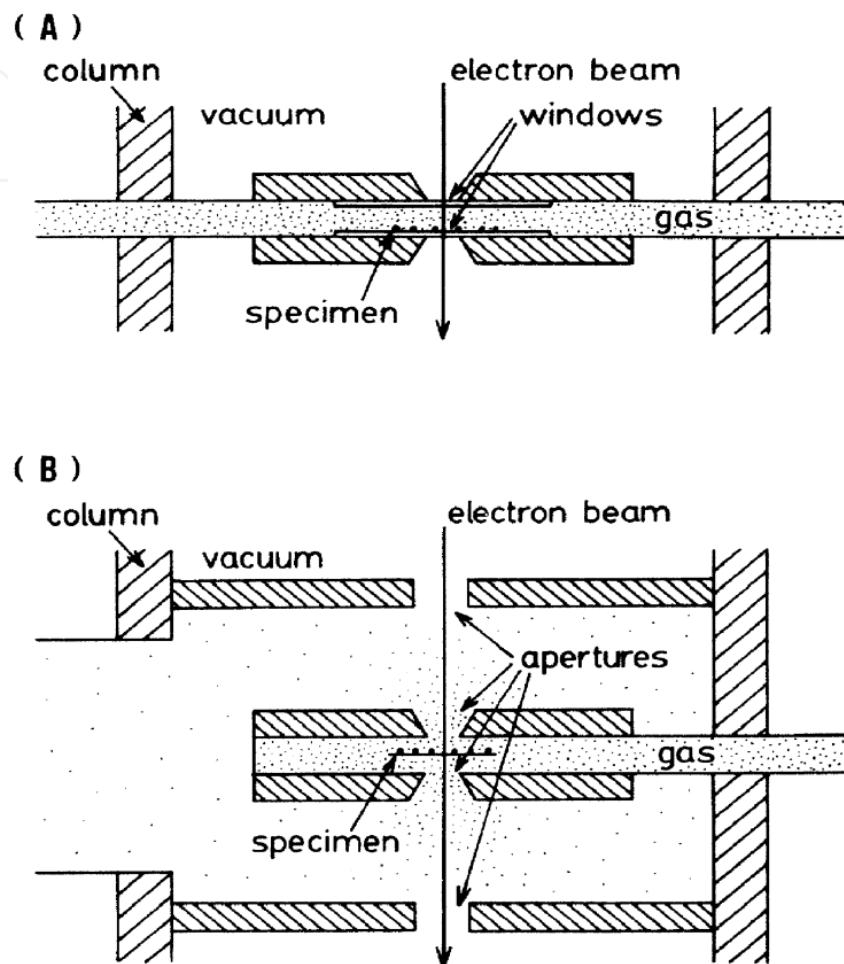

Figure 1. Two types of the EC. (A) Film-sealed EC. (B) Aperture-limited EC. (Fukushima, 1988)

As explained in detail in the following sections, the greatest mystery concerning the mechanism of muscle contraction is how the myosin heads extending from myosin filaments convert chemical energy derived from ATP hydrolysis into mechanical work producing force and motion in muscle. Despite extensive studies, the movement of the myosin heads still remains as a matter of debate and speculation. The reason for the present situation in the field of muscle research arises from the fact that the myosin head movement has been determined only indirectly. The most straightforward way to record the myosin head movement is to observe the myosin head movement in hydrated myosin filaments, which retain their physiological function. In the early 1980's, we had an opportunity to meet Professor Fukami in Nihon University, who succeeded in preparing the carbon sealing film for the film-sealed EC at that time and was looking for coworkers to study physiological function of biological tissues.

We started to work with Fukami's group using the EC, manufactured by the Japan Electron Optics Laboratory (JEOL, Ltd, Co., together with the carbon sealing film developed in Fukami's laboratory. After the period of trials and errors, encompassed over ten years, we succeeded in recording the ATP-induced myosin head movement in hydrated myosin filaments with a number of unexpected findings, which are described in this chapter.

## 2. The gas environmental chamber (EC)

Fig.2 is a schematic diagram of the film-sealed gas environmental chamber (EC). The EC consists of a metal compartment (diameter, 3.5mm; depth, 0.8mm) with upper and lower window frames (copper grids) to pass electron beam. Each window frame has nine apertures, each having a diameter of 0.1mm. The specimen is placed on the surface of lower sealing film, and covered by a thin layer of experimental solution by constantly circulating water vapor through the EC. To obtain clear specimen images, the internal pressure of the EC is made 60—80 Torr. The flow rate of water vapor is adjusted to 0.1—0.2l/min, so that thin layer of experimental solution covering the specimen is in equilibrium with the vapor pressure in the EC (Fukushima et al.,1985; Fukami et al.,1991). The EC was attached to a 200kV transmission electron microscope (JEM 2000EX, JEOL). (Sugi et al.,1997).
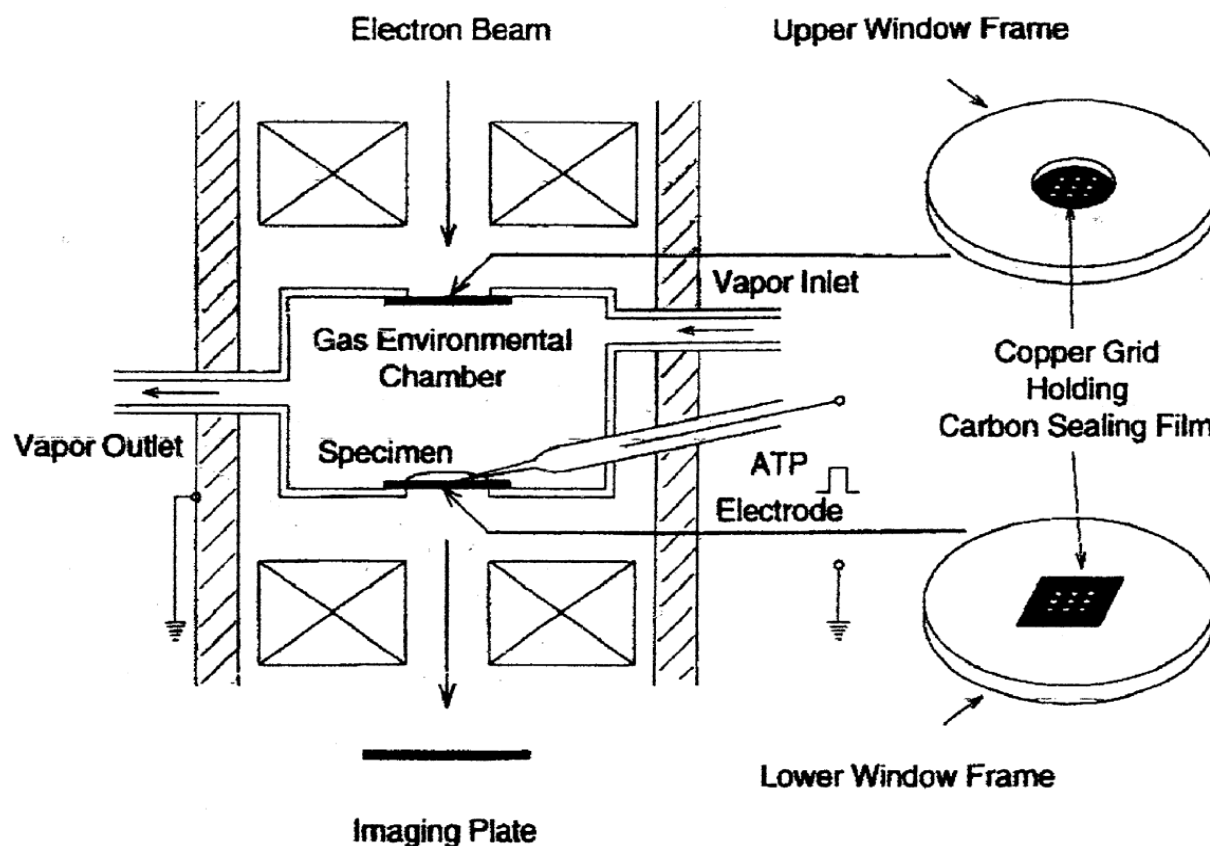
Figure 2. Diagram of the film-sealed EC. The upper and lower windows (copper grids with nine apertures) are covered with carbon sealing films held on copper grids. The EC contains an ATP-containing electrode to apply ATP to the specimen iontophoretically. The image of the specimen is recorded with the imaging plate (IP) (Sugi et al. , 1997).

3. Carbon sealing film

The most important element of the film-sealed EC is the carbon sealing film developed in Fukami's laboratory. In principle, both spatial resolution and contrast of electron micrographs taken by the EC increases with decreasing thickness of the sealing film. Preliminary experiments made in Fukami's laboratory indicated that, to obtain a spatial resolution < 1 nm, thickness of the sealing film should be 15—20nm. Meanwhile, resistivity of a sealing film against pressure difference decreases sharply with increasing its area; the thickness of a sealing film covering a circular aperture of 50μm diameter should be ~100nm to bear a practical pressure difference.
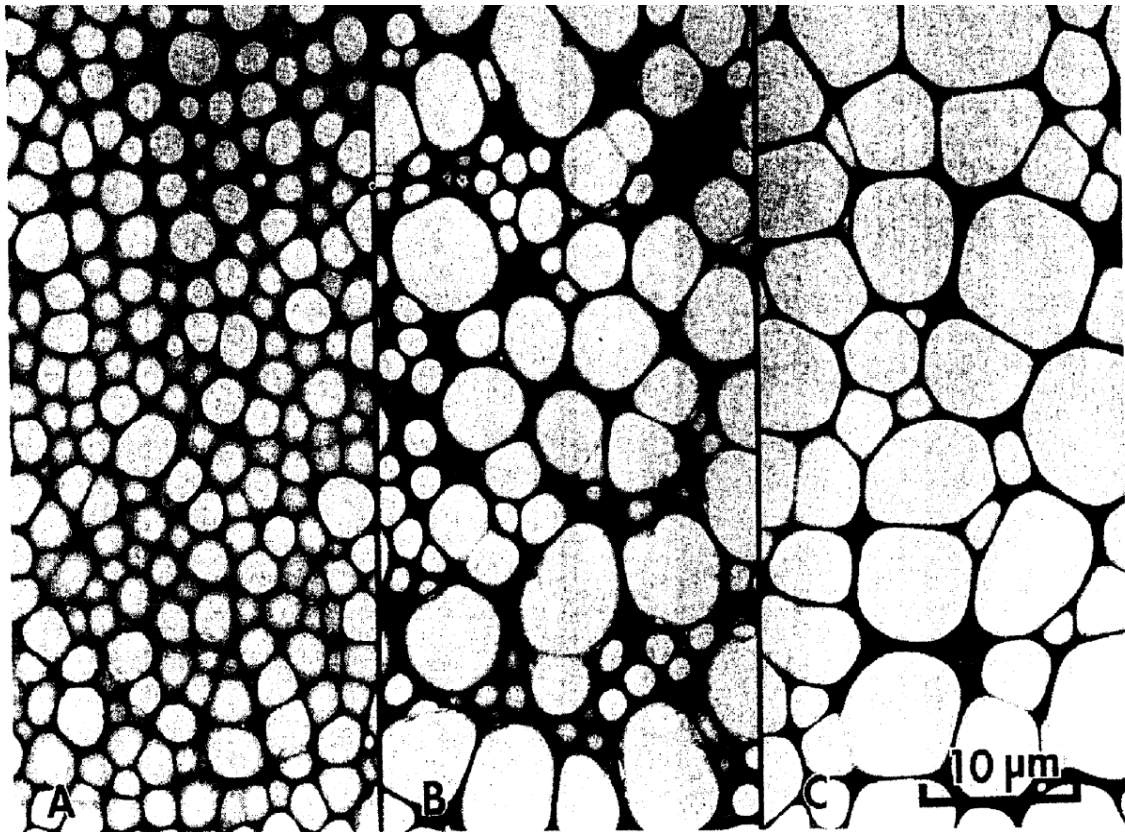

Figure 3. Photomicrographs of plastic microgrides with holes of small diameters (A), with holes of nonuniform diameters (B), and with holes of fairly uniform diameters (5—8nm)(C). (Fikushima, 1988).

As it is practically difficult to a hole < 50μm into metal wall of the EC, Fukami & Adachi (1965) plastic microgrids made from high-molecular organic compound (cellulose acetobutylate). Examples of microgrids are shown in Fig. 3. Microgrids with small (A) or nonuniform holes (B) were unsuitable, while microgrids with fairly uniform holes of 5—8nm diameters (C) were suitable for electron microscopic observation of the specimen.

Fig. 4 illustrates steps to prepare carbon sealing film by covering the microgrid with a thin layer of carbon film (thickness, ~20nm). First, plastic microgrids prepared on a glass slide is put onto water surface (a), where the microgrids (having trapezoidal cross-section) are floating with longer side dounwards (b). The position of the microgrids are inverted by

means of triacetylcellurose (TAC) membrane, and again put oto water surface (c,d). The inverted microgrids are then placed on a mica surface, and exposed to evaporated carbon gas so that the grids are coated with thin carbon layer (e,f). The carbon sealing film prepared on a mica surface are cut into rectangular pieces of appropriate size, and put onto water surface (g,h,i). Finally, pieces of the carbon insulating film is placed onto the copper grid, in such a way that each piece of the insulating film covers nine apertures of copper grid (k).
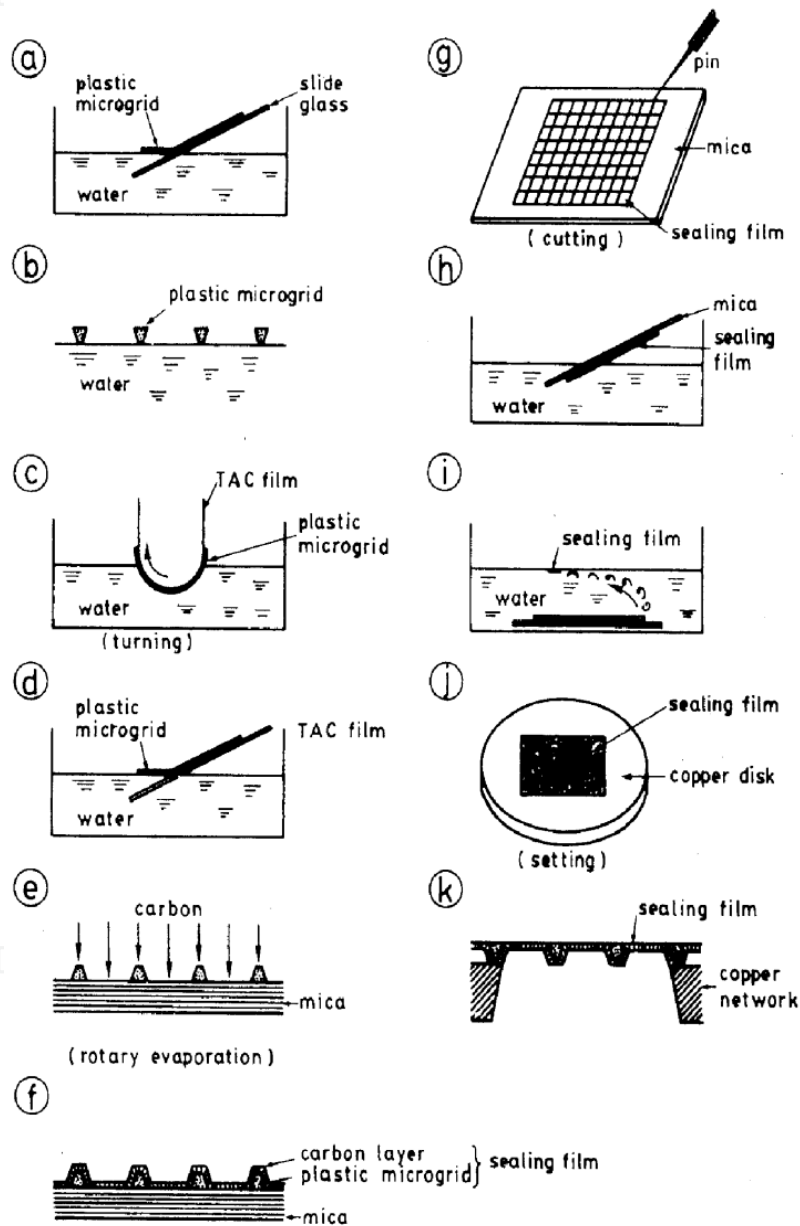

Figure 4. Diagram showing steps to prepare carbon insulating film supported by copper microgrids (Fukushima,1988). For explanation, see text...

The carbon insulating film prepared by the above method well resisted against pressure difference up to 1 atm (Fukushima, 1981).

4. Determination of the critical electron dose to impair function of contractile proteins

Although biological specimens mounted in the EC can be kept in living, hydrated state ,their function is gradually impaired by electron beam irradiation, thus giving a serious limitation in the use of the EC for physiological experiments. Therefore, the critical incident electron dose to impair physiological function of contractile proteins in muscle was determined in by Suda et al. (1992). They observed muscle myofibrils, consisting of hexagonal array of actin and myosin filaments, in the EC (magnification, 2500X), and activated them with ATP.
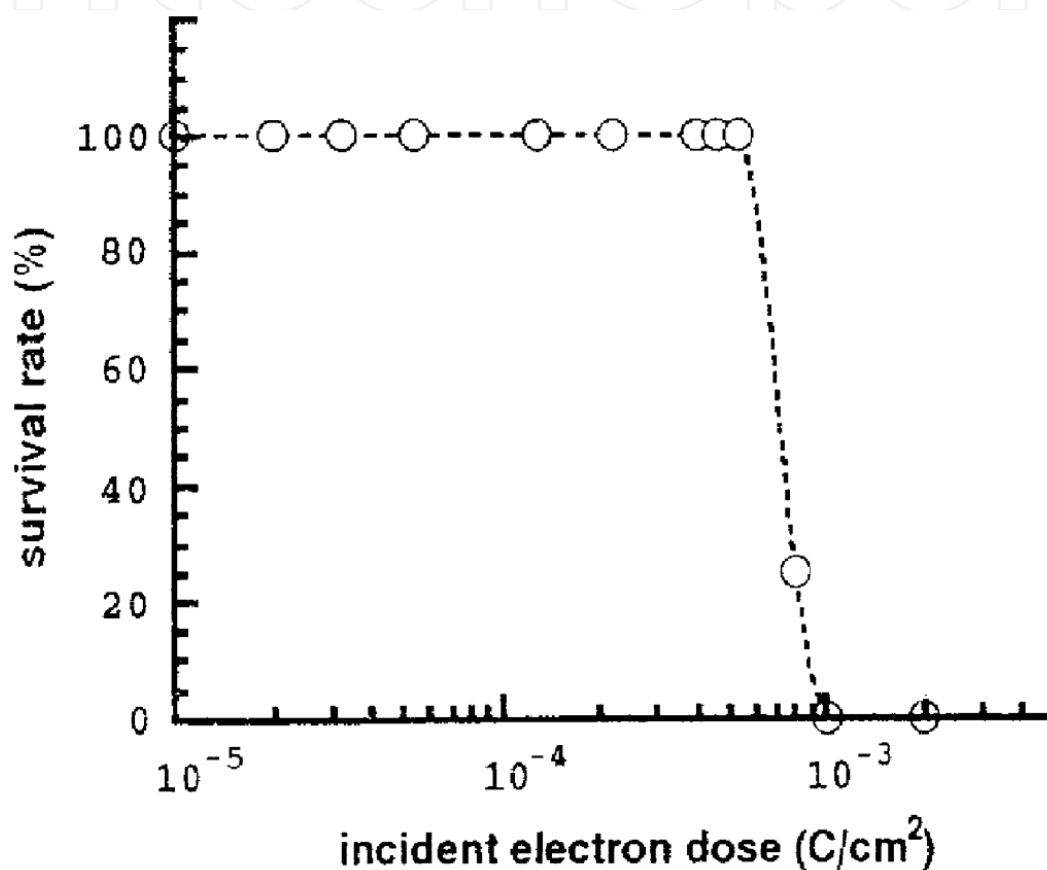
Figure 5. Relation between the total incident electron dose and the survival rate of muscle myofibrils, expressed as percentage of myofibrils contracted in response to ATP in the microscopic field (Suda et al.,1992). Note that contraction of myofibrils in response to ATP disappears when the electron dose exceeds 5×10^{-4} C/cm².

The results are summarized in Fig.5. When the total incident electron dose was $< 5 \times 10^{-4}$ C/cm², all the myofibrils in the electron microscopic field contracted in response to ATP. If, however, the total incident electron dose was further increased, the ATP-induced myofibril contraction disappeared in a nearly all-or-none manner, though the myofibrils showed no appreciable changes in appearance.

The critical electron dose to impair physiological function of contractile proteins was con-firmed by us with respect to both the ATP-induced myosin head movement and the ATPase

activity of hydrated myosin filaments mounted in the EC. Based on these results, electron microscopic observation and recording of the specimen was made with a total incident electron dose < 10^{-4}C/cm^2, being well below the critical dose to impair function of contractile proteins. In order to fulfill this condition, the specimen in the EC had to be observed with extremely weak electron beam intensities (at the fluorescent screen) < 5 x 10^{-13}A/cm^2. Therefore, observation and focusing of the specimen required enormous skill and patience. The electron beam intensity through the specimen under a magnification of 10,000x was 5 x 10^{-13}x $(10,000)^2$ = 5 x 10^{-5}A/cm^2. Immediately after the focusing of the specimen, electron beam was stopped until the time of recording.

5. Background of experiments with the EC

Before describing our experimental results, it seems necessary to give a brief overview of the experimental work to investigate mechanism of muscle contraction. In the middle1950s, H.E. Huxley & Hanson (1954) made a monumental discovery that a skeletal muscle consists of hexagonal lattice of actin and myosin filaments, and that muscle contraction results from relative sliding between actin and myosin filaments (Fig. 6).
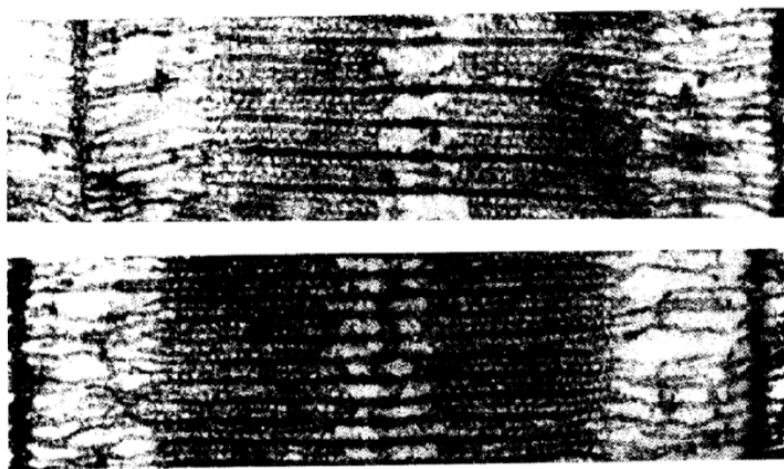

Figure 6. Electron micrographs of longitudinal thin section of rabbi psoas muscle myofibrils (H.E. Huxley, 1957).

Considerable progress has been made with respect to the structure and function of actin and myosin filaments after the discovery of sliding filament mechanism in muscle contraction. As shown in Fig.7A, a myosin molecule is divided into two parts; (1) a long rod called light meromyosin (LMM) and (2) the rest of myosin molecule consisting of a short rod (S2) and two heads (S1) is called heavy meromyosin (HMM). In myosin filaments (or thick filaments), LMM aggregates to form filament backbone, which is polarized in opposite directions on either side of the central part.

While the S1 heads extend laterally from the filament backbone with an axial interval of 14.3nm (Fig.7B). The central part of myosin filament is called the bare region (or bare zone), where the projection of myosin head is absent.
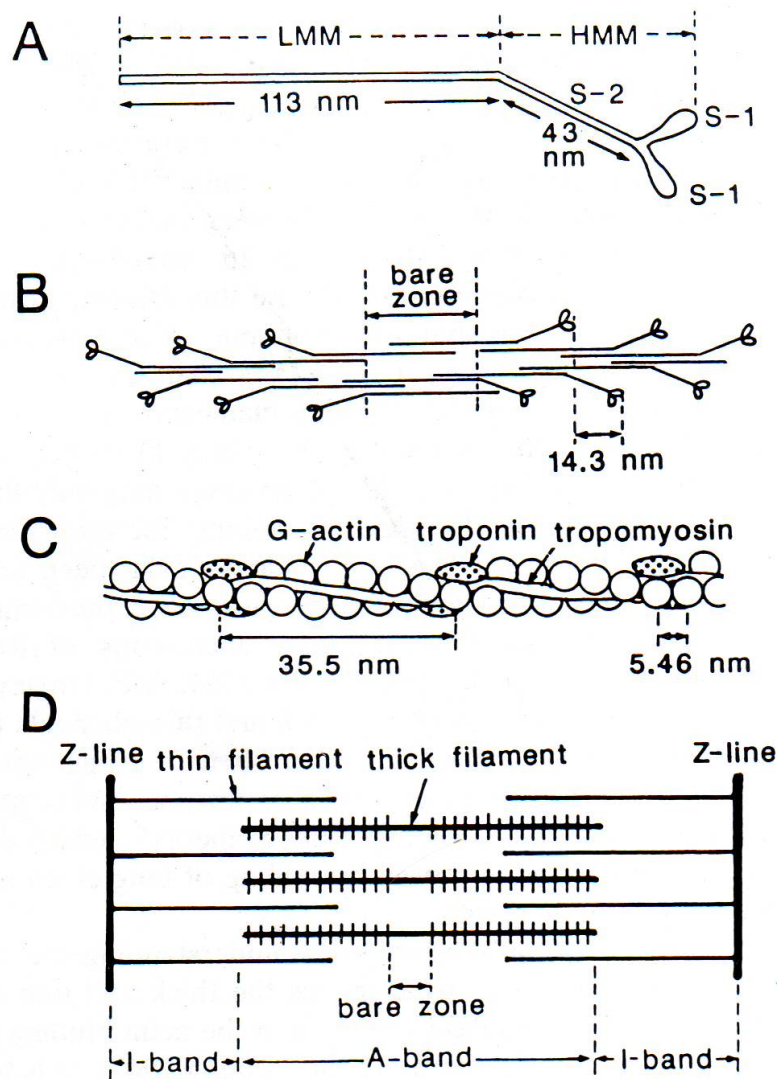
Figure 7. Ultrastructure of myosin (thick) and actin (thin) filaments and their arrangement within a sarcomere. (A) Diagram of a myosin molecule. (B) Arrangement of myosin molecules to form a myosin filament. (C) Arrangement of actin monomers (G-actin) in an actin filament. (D) Longitudinal arrangement of actin and myosin filaments within a sarcomere. Note that the half sarcomere is the structural and functional unit of muscle (Sugi, 1992).

On the other hand, actin filaments consist primarily of two helical strands of globular actin monomers (G-actin) , which are wound around each other with a pitch of 35.5nm. The axial separation of actin monomers in actin filaments is 5.46nm (Fig.7C). In vertebrate skeletal muscle, actin filaments contain tropomyosin and troponin.

As shown in Fig.7D, actin filaments extend from the Z-line to penetrate in between myosin filaments, which are located centrally in each sarcomere. Within a sarcomere, the region containing only actin filaments is called the I-band, whereas the region containing myosin filaments and part of actin filaments is called the A-band. It has been confirmed by a number of experimental methods (H.E. Huxley & Hanson,1954; Page & Huxley,1963; Wray & Holmes,1981) that the filament lengths remain constant irrespective of whether a muscle shortens or being stretched. Therefore, the central problem in understanding the molecular

mechanism of muscle contraction is: what makes actin and myosin filaments slide past each other? Since both actin binding site and ATPase activity are localized in the S1 heads of myosin molecule, it is generally believed that the S1 heads, extending from myosin filament backbone towards actin filaments, play a key role in converting chemical energy of ATP hydrolysis into mechanical work producing force and motion in muscle.
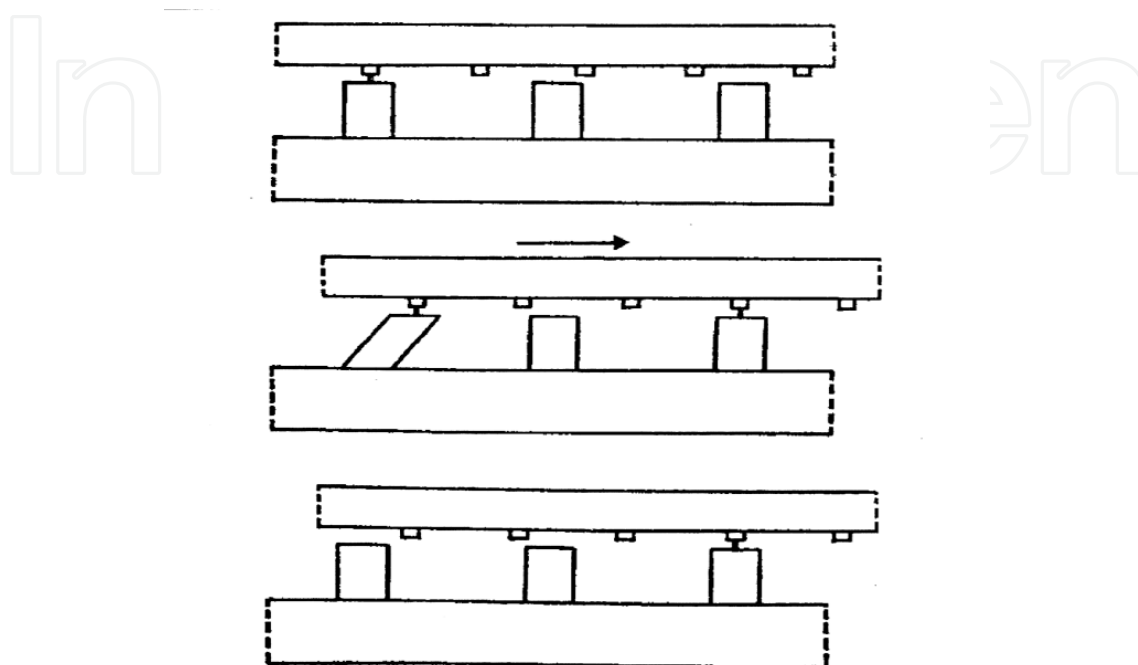
Figure 8. Diagrams showing hypothetical attachment-detachment cycle between the myosin S1 head extending from myosin filament and the sites on actin filament. The myosin head first attaches to actin filament (top diagram), changes its configuration to move actin filament to the right (middle diagram), and then detach from actin filament (bottom diagram). Axial spacing of the myosin heads on myosin filament differs from that of the sites on actin filament, so that the attachment-detachment cycle takes place asynchronously (H.E. Huxley,1969).

Fig.8 illustrates hypothetical attachment-detachment cycle between the S1 heads and the corresponding sites on actin filaments. Extensive studies have been made to prove confor‐ mational changes (or movement) of the myosin heads coupled with ATP during muscle contraction. Although experimental methods used include muscle mechanics, time-resolved X-ray diffraction, chemical probes attached to myosin heads, electron microscopy of quick frozen muscle fibers, and nucleotide-dependent changes of myosin head crystals, no clear conclusion has been obtained (Cooke,1986; Hibbard & Trentham,1986, Geeves & Holmes, 1999, A.F. Huxley,1998).

Thus, the myosin head movement coupled with ATP hydrolysis in muscle still remains to be a matter for debate and speculation. The difficulties in this research field seem to arise from the fact that numerous myosin heads undergo conformational changes asynchronously, so that experimental data are statistical to obscure behavior of individual myosin heads. Since the most straightforward way to study conformational changes in individual myosin heads electron microscopically, we attempted to record ATP-induced movement of individual

myosin head in using the EC, enabling us to keep myofilaments in hydrated, living state. As described later, the EC has been proved to be extremely powerful tool in visualizing the behavior of individual myosin heads under the electron microscope with high magnifications.

6. Experimental methods

In order to achieve the purpose to record movements of myosin head in hydrated myosin filaments, the following problems in experimental technique had to be solved: (1) how to record images of the specimen with extremely weak electron beam intensities, (2) how to position-mark myosin heads without specimen staining used for conventional electron microscopy; and (3) how to apply ATP to the specimen without changing its position in the electron microscopic field. We solved these problems in the following ways.

6.1. Recording of specimen image

Based on the critical electron dose to impair function of contractile proteins (Fig.5), experiments were performed under electron microscopic magnification of 10,000x, and the specimen images were recorded on an imaging plate (IP) system (PIX system, JEOL). The IP is 10.2 x 7.7cm in size, and has a sensitivity ~60times that of X-ray film. The exposure time was 0.18s with an electron beam intensity of $1—2 \times 10^{-12}$A/cm^2. The number of pixels in the IP is ~12,000,000 to give a special resolution mdose, recording of the specimen image can only be repeated at most 4times. The IP system was developed by Fuji Photofilm Co., and is now used worldwide not noly for transmission electron microscope, but for other purposes like time-resolved X-ray diffraction.

6.2. Preparation of synthetic bipolar myosin filaments and position marking of myosin heads

We decided to use synthetic thick filaments, consisting of myosin-myosin rode mixture, prepared from rabbi psoas muscle. Myosin was prepared by the method of Perry (1955), while myosin rod was obtained by chymotryptic digestion of myosin by the method of Margossian & Lowey (1982). Myosin and myosin rod were mixed at a molar ratio of 1:1, and were slowly polymerized by dialysis against a solution of low ionic strength (KCl concentration, 120mM) to bipolar myosin filaments (1.5—3μm in length, and 50—200nm in diameter at the center) suitable for our experiments. As shown in Fig. 9, the synthetic filaments are spindle-shaped, and their polarity is reversed across their central region, as judged from the direction of extension of rod part of HMM (myosin S2) from the filaments. Though the myosin S1 heads are lost from the filaments, probably due to fixation and staining procedures, this indicates that the synthetic filaments are bipolar in structure, being similar to native myosin filaments in muscle.

To position-mark individual myosin heads in the hydrated myosin filaments without staining procedures, colloidal gold particles (diameter, 20nm; coated with protein A; EY labora-

tories) were attached to the myosin heads, using a site directed antibody (IgG) to the junctional peptide between 50- and 20-kDa segments of myosin heavy chain (Sutoh et al.,1989). The antibody attaches to only one of the two myosin heads near its distal end facing actin filaments. Technical details to position-mark individual myosin heads have been described elsewhere (Sugi et al., 1997). It was essential to position-mark myosin heads sparsely, so that each gold particle was reasonably separated from neighboring particles.

Figure 9. Conventional electron micrograph of synthetic bipolar myosin filaments. Note that the direction of extension of rod part of HMM (myosin subfragment 2) from the filaments is reversed across their central region

6.3. Application of ATP to the specimen

To apply ATP to the specimen without causing its displacement, we used conventional glass capillary microelectrodes containing 100mM ATP (see Fig.2). By passing current pulses through the electrode, negatively charged ATP ions are moved out of the electrode. The iontophoretically released ATP ions from the electrode reach to the specimen by diffusion in the experimental solution covering the specimen. Normally, a rectangular current pulse (intensity, 10nA; duration, 1s) from an electronic stimulator was applied to the electrode through a current clamp circuit (Oiwa et al.,1993). Total amount of ATP released from the microelectrode was estimated to be ~10—14mol (Oiwa et al.,1991). The time required for the released ATP to reach the specimen by diffusion was estimated to be <30s by video recording

ATP-induced shortening of myofibrils in the EC under a light microscope. Hexokinase (50units/ml) and D-glucose (2mM) were added to the experimental solution to eliminate contamination of ATP (Oiwa et al.,1991). In some experiments, ADP was also applied to the specimen with similar method.

6.4. Data analysis

Under an electron microscopic magnification of 10,000x, the pixel size on the IP is 2.5 x 2.5nm. In our experimental condition, the number of electrons reaching each pixel is esti-mated to be at most 7—8. Each IP record of the specimen was divided into a number of subframes, and each subframe was observed on the monitor screen of electron microscope. Due to electron statistics, the shape of gold particle images was variable. Particles with near-ly circular shape were selected to be used for analysis, after an appropriate binning proce-dure, i.e. the procedure to determine each particle configuration consisting of particles with electron counts above a certain level. Particle shapes were not markedly altered by the level of binning.

Then, the center of mass position of each selected gold particle was determined with an image processor (Nexus Qube System, Nexsus) in the early experiments, and with an ordi-nary personal computer in the late experiments. The center of mass position was obtained as the coordinates (two significant figures) within a single pixel where the center of mass posi-tion was located, and the coordinates, representing the position of the particle, were also taken to represent the position of the myosin head. The position of the myosin head, deter-mined by the above method, was compared between the two IP records. The absolute coor-dinates common to the two IP records were obtained from the position of natural markers, i.e. bright spots on the carbon sealing film. When the center of mass position was different between the two IP records, the distance (D) between the two center of mass positions (with the coordinates X1 and Y_1 and X2 and Y2, respectively) was calculated as $D = \sqrt{(X1-X2)^2 + (Y1-Y2)^2}$, and this value was taken as the amplitude of myosin head movement.

7. Experimental results and their interpretation

Prior to the experiments to be described in the following sections,we first made experiments with the EC using myosin-paramyosin hybrid filaments, in which rabbit skeletal muscle myosin was bound around the surface of long and thick paramyosin filaments obtained from molluscan somatic smooth muscle, because this hybrid filaments were very easy to handle experimentally. Although we established our experimental methods already de-scribed in the preceding sections during the course of experiments, and succeeded in record-ing the ATP-induced myosin head movement (Sugi et al.,1997), we do not mention the re-sults obtained on this hybrid filaments because (1) the space available for this chapter is limited, and (2) the results obtained from the unusual material may not attract attention of general readers.

7.1. Stability of myosin head position in the absence of ATP

Fig.10 shows examples of spindle-shaped bipolar myosin filaments with a number of gold particles bound to individual myosin heads. The particle image consisted of 20—50 dark pixels with a wide range of gradation, reflecting electron statistics. We first examined

whether the particle position, representing the myosin head position, was stable or changed with time in the absence of ATP, by comparing the center of mass position of the same parti‐ cle between the two IP records of the same filament, taken at an interval of 5—10min, and then the two IP records were superimposed to detect differences in particle position.
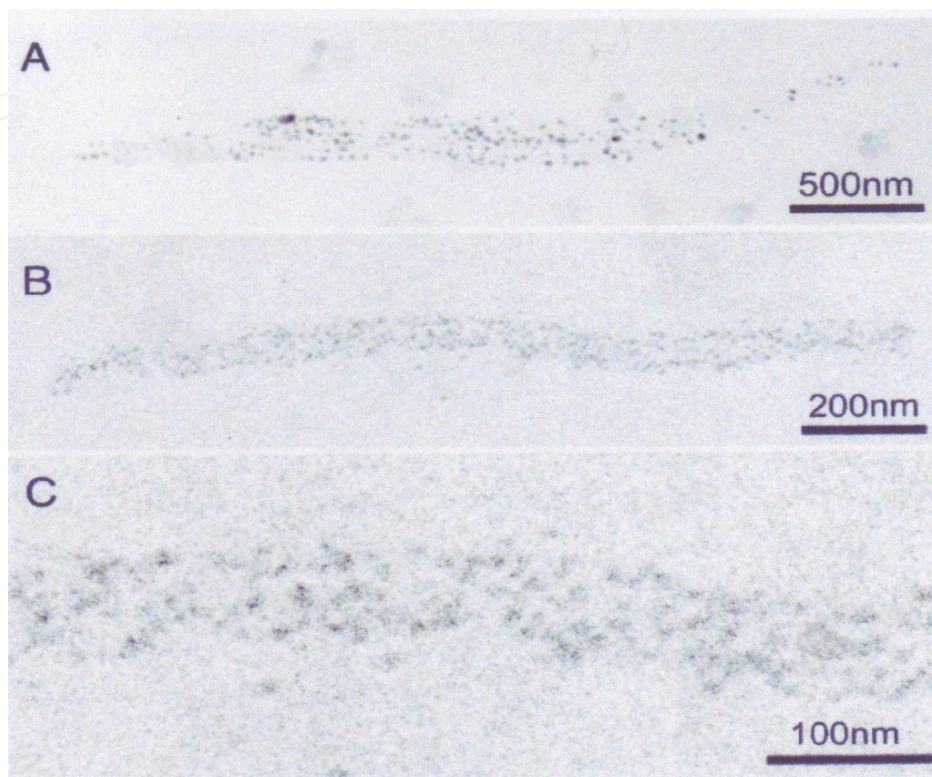

Figure 10. (a and b) Examples of IP records of single bipolar myosin filaments with a number of gold particles attached to individual myosin heads. (c) Enlarged view of myosin filament shown in (a) (Sugi et al.,2008).

An example of superimposed tracings of the two IP records is presented in Fig. 11a, in which open and filled circles of 20nm diameter are drawn around the center of mass posi‐ tion of particles in the first and the second records, respectively. It was found that filled circles in the second record are almost completely covered by open circles in the first record. This indicates that (1) the filament stick firmly to the surface of carbon sealing film, and that (2) the position of individual myosin heads on the filament remain almost unchanged with time. Fig.11b is a histogram showing distribution of the distance between the center of mass positions of particles in the first and the second records. Among 120 particles on three dif‐ ferent pairs of IP records, 93 particles exhibited no significant changes in position ($D < 2.5nm$), while the rest 27 particles showed only small position changes ($2.5nm < D > 5nm$).

The stability in position of both the filament and the myosin heads in the absence of ATP pro‐ vided an extremely favorable condition for recording the myosin head movement in response to applied ATP. Although individual myosin heads are believed to continue thermal fluctua‐ tion, their mean position, time-averaged over the exposure time of IP recording (0.18s), re‐ mains almost unchanged with time. Since the same stability of myosin heads has also been

observed in the hybrid filaments (Sugi et al.,1997), the stability in time-averaged myosin head mean position seems to be common to myosin heads extending from myosin filament in all kinds of muscle, and is consistent with the contraction model of A.F. Huxley, in which each myosin head fluctuates around a definite equilibrium position (A.F. Huxley, 1957).
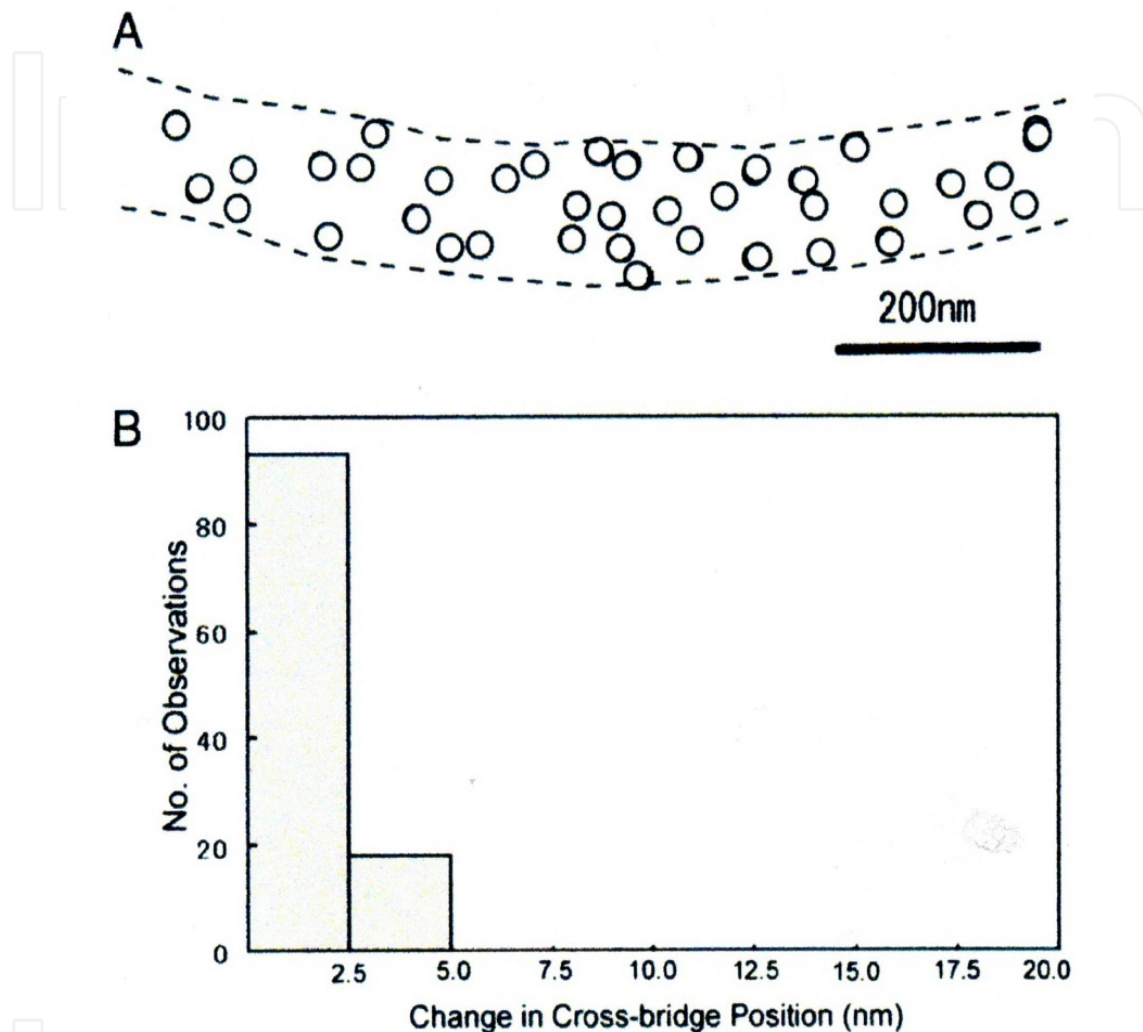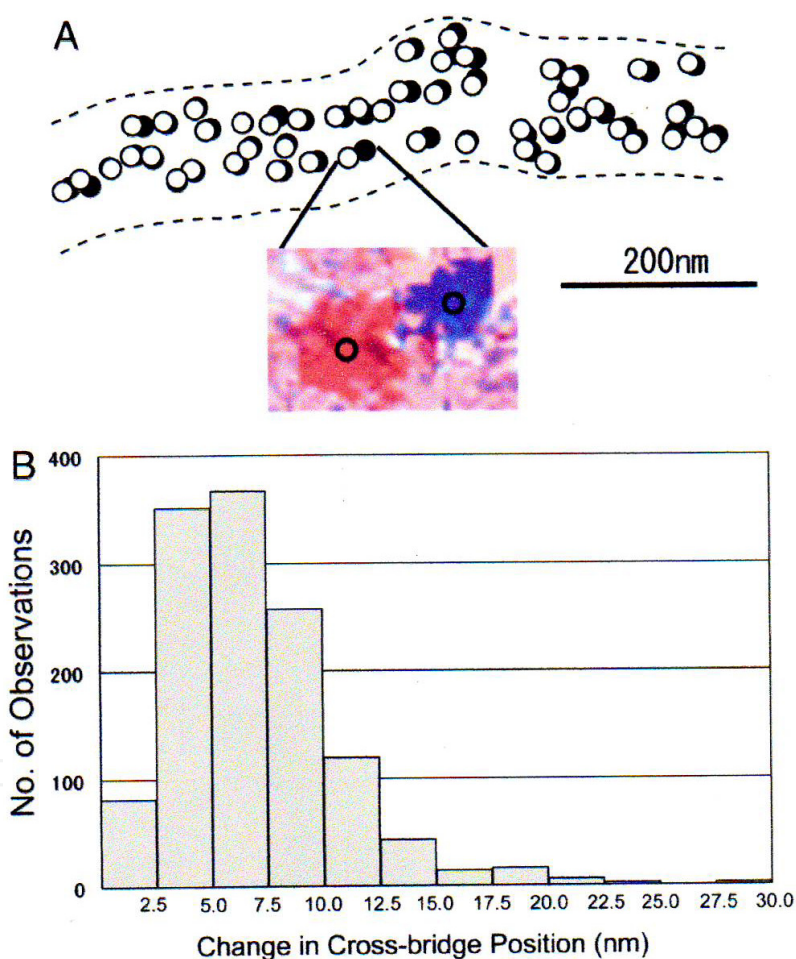

Figure 11. Stability of time-averaged myosin head position in the absence of ATP. (a) Comparison of the myosin head position between the two IP records of the same filament. Open and filled circles (diameter, 20nm) are drawn around the center of mass position of each particle in the first and the second IP records, respectively. In this and subsequent figures, broken lines indicate contour of the filament. Note that filled circles are barely visible because of almost complete overlap of open circles over filled circles. (b) Histogram showing distribution of distance between the center of mass positions of particles in the first and the second IP records (Sugi et al.,2008). Note also that, in Figs. 11 and 12, the term, cross-bridge, is used instead of the term, myosin heads.

7.2. ATP-induced myosin head movement

On the basis of the stability of time-averaged myosin head mean position with time, we explored myosin head movement in response to iontophoretically applied ATP, by comparing two IP records of the same filament, one taken 3—4min before while the other

taken 40—60s after ATP application. Since it was not easy to focus part of myosin filament including the bare region (see Fig.7B) within the critical electron dose to impair function of myosin molecules, we first examined ATP-induced myosin head movement at one side of the bare region.

After ATP application, the position of individual myosin heads on the filament was found to move in one direction nearly parallel to the filament long axis, as shown in Fig. 12a (Sugi et al.,2008). Fig. 12b is a histogram showing distribution of the amplitude of ATP-induced myosin head movement, constructed from 1,285 measurements on 8 different pairs of IP records obtained from 8 different myosin filaments. The histogram exhibited a peak at 5—7nm, and the average amplitude of myosin head movement was 6.5±3.7nm (mean±SD, (n=1,210).
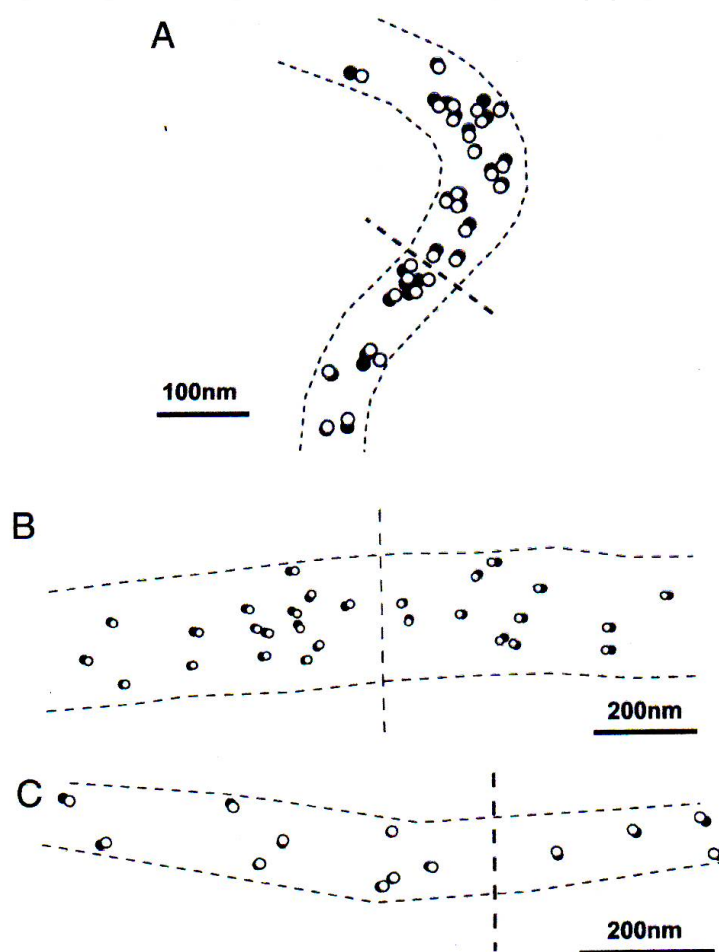

Figure 12. ATP-induced myosin head movement. (a) Comparison of the myosin head position between the two IP records. Open and filled circles (diameter, 20nm) are drawn around the center of mass positions of the same particles before and after ATP application, respectively.

(Inset) an example of superimposed IP records showing the change in position of the same particle, before (red) and after (blue) ATP application. (b) Histogram showing distribution of the amplitude of ATP-induced myosin head movement, determined from changes in the center of mass position of each particle (Sugi et al.,2008).

In our experimental condition, gold particles located on both upper and lower side of the filaments were equally in focus in the microscopic field. The myosin heads on the filament upper side may move freely in response to ATP, while the movement of myosin heads on the lower side of the filament may be largely or completely inhibited due to firm attachment of the filament to the carbon sealing film. If this explanation is correct, the mean amplitude of ATP-induced movement of myosin heads that can move freely would be > 7.5nm. As has been the case in the previous study (Sugi, 1997), the ATP-induced myosin head movement was eliminated by treatment with N-ethylmaleimide, indicating that the myosin head movement is associated with its reaction with ATP.

Figure 13. Examples of IP records showing the ATP-induced myosin head movement at both sides of the myosin filament bare region, across which the myosin head polarity is reversed. Open and filled circles (diameter, 20nm) are drawn around the center of mass positions of the same particles before and after ATP application, respectively. Note that the myosin heads move away from the bare region, indicated by vertical broken lines (Sugi et al., 2008).

7.3. Direct demonstration of myosin head recovery stroke

After enormous painstaking efforts, we finally succeeded in recording the ATP-induced myosin head movement at both sides of the myosin filament bare region, across which the

myosin head polarity was reversed (see Figs. 7 and 9). It was found that, on application of ATP, myosin heads moved away from the bare region. Typical examples of IP records showing the reversal in the direction of myosin head movement are presented in Fig. 13.

Fig. 14 is a diagram illustrating generally accepted view on the attachment-detachment cycle between the myosin head (M) extending from myosin filament and actin monomer (A) in actin filament, based on biochemical studies on the kinetics of actomyosin ATPase reaction in water solution (Lymn & Taylor, 1971). M in the form of complex, M · ADP · Pi, attaches to A (A), and exerts a power stroke, associated with release of Pi and ADP (from A to B). After the end of power stroke, M remains attached to A, taking its post-power stroke configuration (B). Upon binding with ATP, M detaches from A, and exerts a recovery stroke, associated with reaction, M · ATP → M · ADP · Pi (from C to D). Then M · ADP · Pi again attaches to A (from D to A) and the cycle is repeated.

Though our experimental system does not contain actin filaments, it seems likely that myosin heads before ATP application may take configurations analogous to those at the end of power stroke (B in Fig. 14), and in response to applied ATP, they bind with ATP to form complex M · ADP · Pi, which is known to have average lifetime > 10s due to its slow Pi release (Lymn & Taylor,1971). Therefore, majority of myosin heads in the IP record, taken after ATP application, may be in the state of M · ADP · Pi, suggesting that the ATP-induced myosin head movement, recorded in our EC experiments, is coupled with reaction, M + ATP → M · ADP · Pi, and therefore may correspond to the recovery stroke (C to D, in the diagram of Fig. 14.
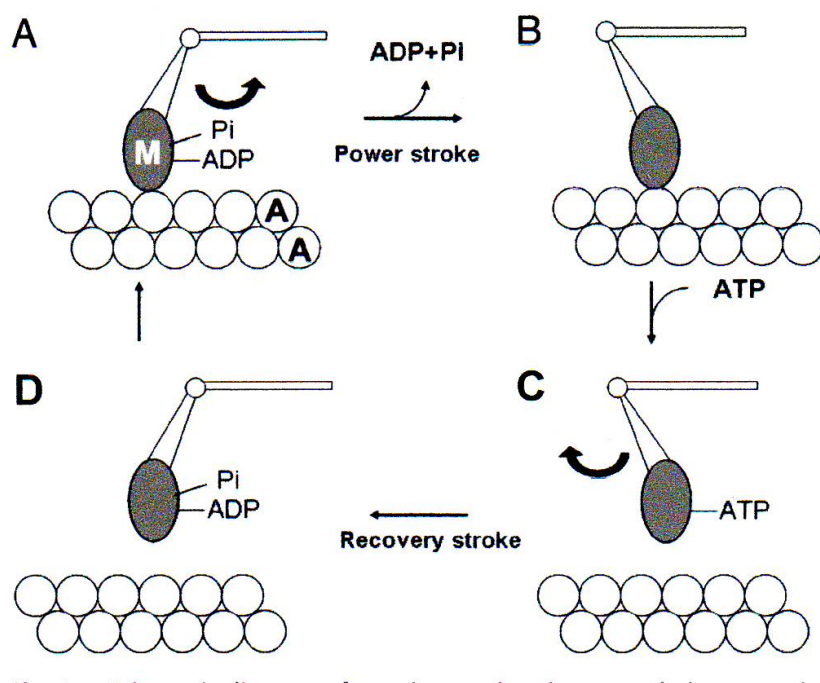
Figure 14. Diagram of the attachment-detachment cycle between myosin head (M) extending from myosin filament and actin monomer (A) in actin filament, based on biochemical studies on actomyosin ATPase reactions. For further explanations, see text. (Sugi et al.,2008).

In order that myosin heads in muscle repeat attachment-detachment cycles with actin filaments, the recovery stroke should be the same in amplitude as, but opposite in direction to, the power stroke, in which myosin heads should move towards the bare region of myosin filament. As a matter of fact, myosin heads that had moved away from the filament bare region, were found to return to their initial position after exhaustion of applied ATP with hexokinase and D-glucose serving as ATP scavenger.

Fig. 15 illustrates 9 examples of superimposed IP records, each record showing sequential changes in location of the pixels (2.5 x 2.5nm), in which the center of mass position of the corresponding gold particles is included. Red, blue and yellow pixels in each record indicate the center of mass positions of the same particle before ATP application, during ATP application, and after complete exhaustion of applied ATP, respectively. It can be seen that myosin heads returned exactly to their initial position in records a, b and i, and close to their initial position in records c to h. The return of myosin heads to their initial position may be associated with reaction, $M \cdot ADP \cdot Pi \rightarrow M + Pi + ADP$, i.e. detachment of Pi and ADP from M. In the presence of actin filaments, this reaction corresponds to the myosin head power stroke (A to B in Fig.14).

To summarize, our findings on the ATP-induced myosin head movement in hydrated, living myosin filaments constitute the first direct demonstration of the myosin head recovery stroke. On the other hand, the return of myosin head to their initial position after exhaustion of applied ATP is not regarded to correspond to myosin head power stroke at present, as our experimental system does not contain actin filaments. Nevertheless, our results may be taken to indicate that, even in the absence of actin filaments, individual myosin head can exhibit cyclic movement coupled with ATP hydrolysis. In other words, individual myosin heads can perform cyclic movement analogous to that shown diagrammatically in Fig.14 without being guided by actin filaments. Recently, we have succeeded in recording the myosin head power stroke in the presence of actin filaments, and are obtaining extremely interesting preliminary results, further proving that the EC is a powerful tool in making breakthroughs in the field of molecular mechanism of muscle contraction.

8. Electron microscopic evidence for lever arm mechanism of myosin head movement

At the end of this chapter, we will describe our recent piece of work with EC concerning the myosin head lever arm mechanism. Fig. 16 is a diagram showing molecular structure of the myosin head, consisting of catalytic domain CAD) containing actin binding and ATPase sites, and lever arm domain (LD), connected to myosin filament backbone via myosin sub-fragment 2 (S2). The two domains are connected by small, flexible converter domain (CD). Mainly based on crystallographic studies on nucleotide-dependent structural changes in myosin head crystals, which are detached from myosin filaments (Geeves & Holmes,1999), it has been suggested that the myosin head power stroke is produced by active rotation of LD around CD, while CAD remains rigid. It is not clear, however, whether the myosin head

power stroke is actually produced by the above lever arm mechanism in muscle, in which the myosin heads are not detached from, but are firmly connected to, myosin filament backbone.
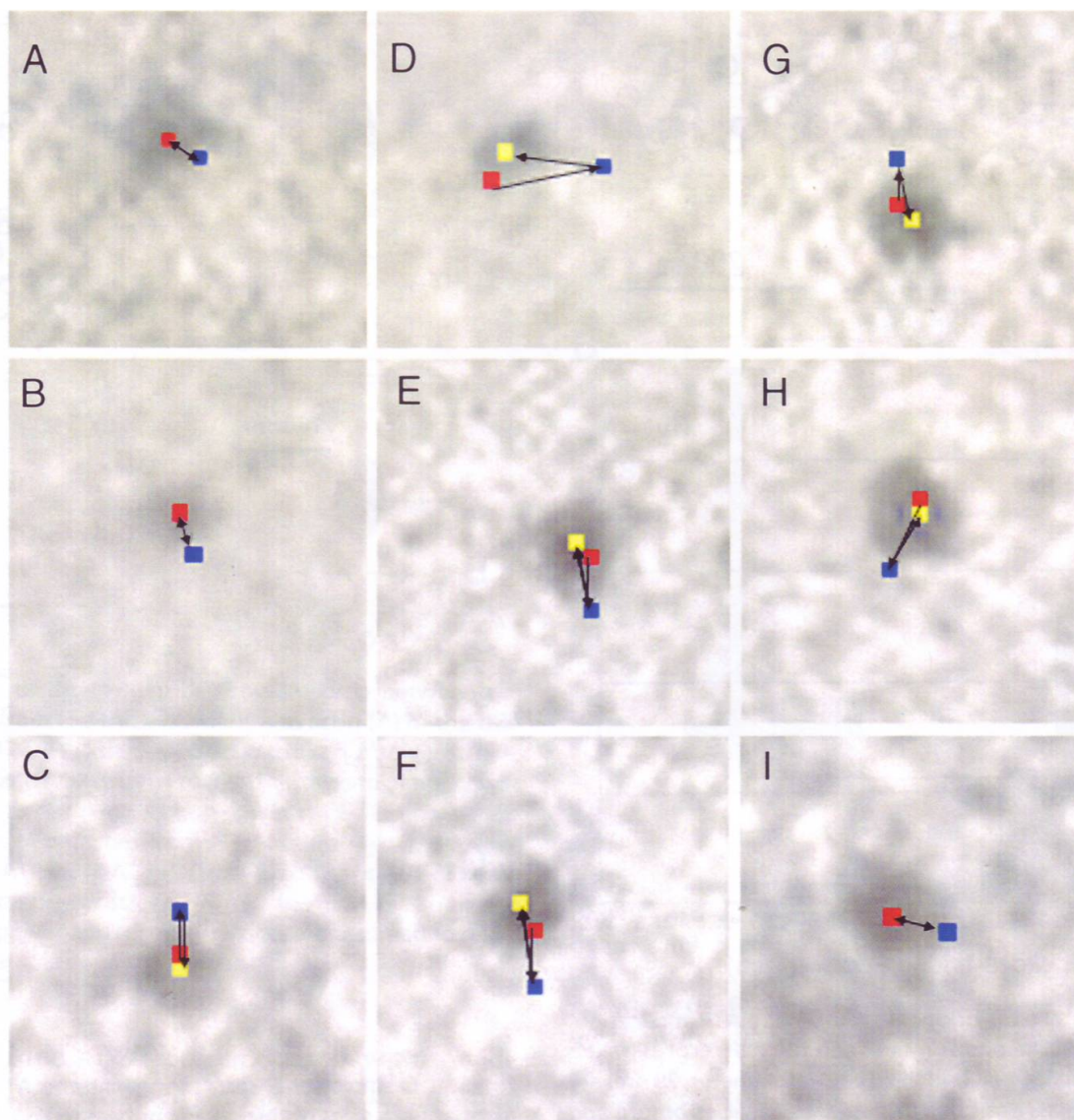
Figure 15. Examples showing sequential changes in position of 9 different pixels (each 2.5 x 2.5nm) where the center of mass positions of corresponding 9 particles are located. In each frame, pixel positions before ATP application (red), during ATP application (blue), and after exhaustion of ATP (yellow) are indicated. Note that myosin heads return towards their initial position after exhaustion of applied ATP (Sugi et al.,2008).

To give answer to this question, we prepared three different monoclonal antibodies (IgG) directed to three different regions within a single myosin head. Antibody 1 is identical with that used in our previous experiments already described in this chapter, and attaches to junctional peptides between 50k and 20k segments of myosin heavy chain. Antibody 2 attaches around reactive lysine residue (Lys 83) in CD. Antibody 3 attaches to two peptides (Met 58—Ala 70 and Leu 106−Phe 120) in myosin regulatory light chain in LD. The ATP-

induced movement at three different parts within individual myosin heads was recorded using myosin filaments with myosin heads position-marked with antibodies 1, 2 or 3 and 3' by the method previously described.
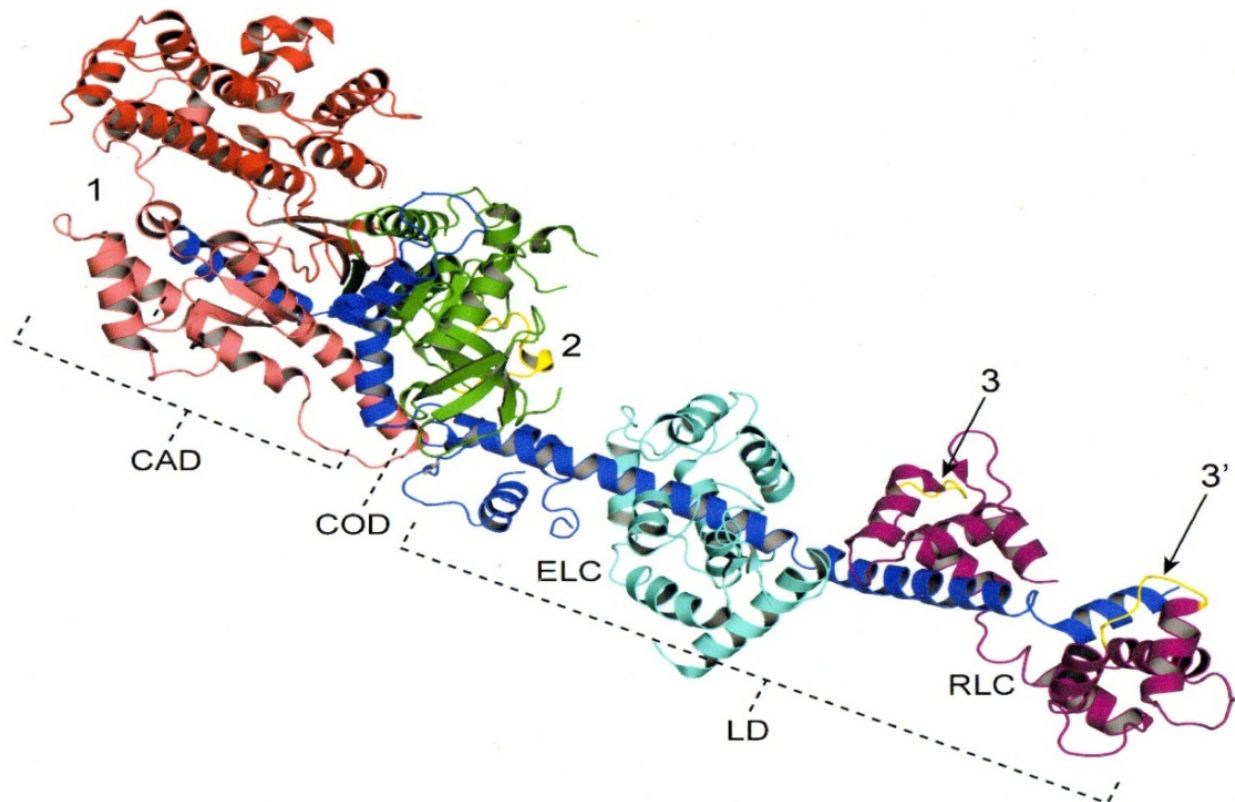

Figure 16. Myosin head structure showing approximate regions of attachment of antibody 1, 2 and 3, indicated by numbers 1, 2 and 3, respectively. The catalytic domain (CAD) comprises 25k (green), 50k (red) and part of 20k (dark blue) fragments of myosin heavy chain, while lever arm domain (LD) comprises the rest of 20k fragment and essential (ELC, light blue) and regulatory (RLC, magenta) light chains. CAD and LD are connected via converter domain (CD). Location of peptides around Lys 83 and that of two peptides (Met 58—Ala 70 and Leu 106—Phe 120) in LD are colored yellow. Regions of attachment of antibodies 1,2 and 3 are indicated by numbers 1, 2 and 3 and 3', respectively (Minoda et al.,2011).

Fig. 17 illustrated the results obtained as well as their interpretation. As can be seen in the three histograms. Fig. 17A, B and C are histograms of amplitude distribution of ATP-induced movement of myosin heads, position-marked with antibody 1, antibody 2 and antibody 3, respectively. The mean amplitude of ATP-induced movement was 6.14±0.09 (mean±s.e.m., n =1,692) at the distal part of CAD (A), and 6.14±0.22 (n = 1,112) at the CAD-CD boundary (B), indicating no significant difference between the two extreme regions of CAD. On the other hand, the average amplitude of ATP-induced movement at the regulatory light chain in LD was 3.55±0.11nm (n = 981), being significantly smaller than the corresponding values in CAD (t-test, P < 0.01).

If it is assumed that the cyclic conformational changes of myosin heads in the absence of actin filaments (Fig.17D) are in principle similar to the conformational changes of myosin

heads in the presence of actin filaments in muscle (Fig.17E), the results shown in Fig.17 A—C can be accounted for by the lever arm mechanism in the following way.
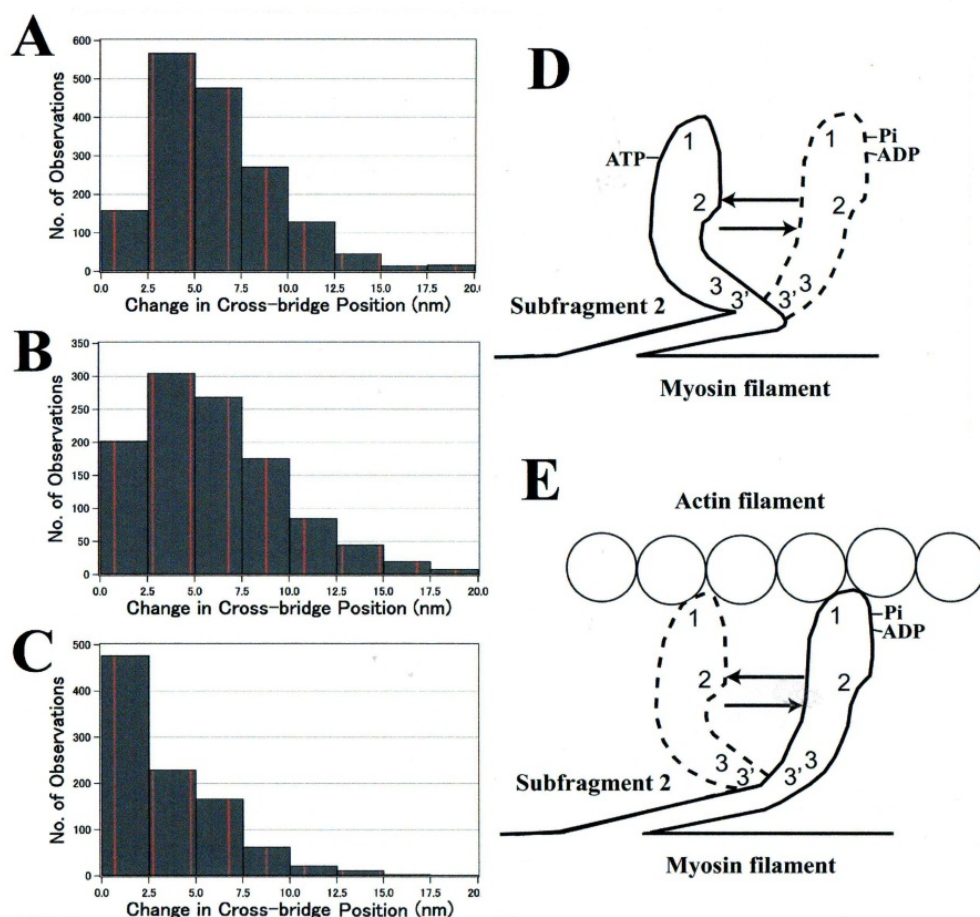
Figure 17. (A—C) Histograms showing amplitude distribution of ATP-induced myosin head movement, position-marked with antibody 1 (A(, antibody 2 (B), and antibody 3,3, respectively. (D,E) Diagrams illustrating myosin head lever arm mechanism in the absence (D) and in the presence (E) of actin filament. Attachment regions of 'of antibodies 1, 2 and 3 are indicated by numbers 1, 2 and 3,3', respectively (Minoda et al.,2011).

In the absence of actin filaments, the myosin head is initially thought to be in the post-power stroke configuration (solid line in D), and on binding with applied ATP it changes its conformation to reach the post-power stroke configuration with bound ATP hydrolysis products(Pi and ADP) (broken line in D). During this recovery stroke, the myosin head lever arm domain rotates not only around the converter domain, but also around the boundary between the lever arm domain and myosin S2, connecting the myosin head to myosin filament backbone. As a result, the amplitude of ATP-induced movement is definitely larger at both the distal and the proximal end of myosin head catalytic domain (indicated by numbers 1 and 2) than at the regulatory light chain in myosin lever arm domain (3 and 3').

During the myosin head power stroke taking place in muscle, the myosin head is initially in the pre-power stroke configuration with bound Pi and ADP, and attaches to actin filament

(solid line in E). Then it undergoes power stroke releasing Pi and ADP, to take the post-power stroke configuration (broken line in E). To summarize, the measurement of ATP-induced movement at three different parts within individual myosin is not only consistent with the myosin head lever arm mechanism to produce force and motion in muscle, but may also constitute the first success in recording local structural changes taking place within a single macromolecule.

9. Conclusion

The experiments described in this chapter have proved that the EC is an extremely powerful tool in elucidating fundamental mysteries remaining in the research field on molecular mechanism of contraction. The greatest advantage of the use of EC for investigating muscle contraction is that it enables us to record movement of individual myosin heads coupled with ATP hydrolysis in hydrated myosin filaments, which retain their physiological function in an electron microscope.

In contrast, all other experimental methods hitherto used by a number of investigators, including time-resolved X-ray diffraction and chemical probe experiments (Cooke,1986; Hibbard & Trentham,1986), to study myosin head movement can only obtain averaged values since these methods inevitably sample numerous number of myosin heads acting asynchronously. Crystallographic and electron microscopic studies on myosin S1 crystal and acto-S1 complex (Geeves & Holmes,1999) are also concerned only with static structures and the results obtained are also statistical in nature. We believe that our work using the EC has made a breakthrough to open new horizon in this research field. As a matter of fact, we have already succeeded to study the myosin head power stroke in hydrated myosin filaments in the presence of actin filaments. A preliminary report of this work has appeared (Minoda et al.,2011).

Finally, we emphasize that the EC can be used not only for muscle research, but also for a number of other research fields to study function of biomolecules. We heartily hope that the EC will be used widely by life scientists to elucidate various mysteries in their respective research field. The EC system (JEOL,Ltd) is commercially available, and can be attached to any 100 or 200kV transmission microscope. Those who are interested in the carbon insulating film may consult JEOL or H.S. (sugi@kyf.biglobe.ne.jp) about its preparation.

Author details

Haruo Sugi[*]
Department of Physiology, School of Medicine, Teikyo University, Japan

Hiroki Minoda
Department of Applied Physics, Tokyo University of Agriculture and Technology, Japan

Takuya Miyakawa and Suguru Tanokura
Graduate School of Agriculture and Science, University of Tokyo, Japan

---

[*] Corresponding Author

Shigeru Chaen
Department of Human and Engineered Environmental Studies, Nihon University, Japan

Takakazu Kobayashi
Department of Electronic Engineering, Shibaura Institute of Technology, Japan

Acknowledgement

10. References

Buttler, E.P. & Hale, K.F.(eds) (1981). Dynamic Experiments in the Electron Microscope. In: *Practical Method in Electron Microscopy* Vol.9, North Holland, Amsterdam

Cooke, R. (1986). The mechanism of muscle contraction. CRC critical Reviwes in Biochemistry 21: 53—118

Fukami, A. & Adachi, K. (1965). A new method of preparation of a self-perforated microplastic grid and its applications. Journal of Electron Microscopy (Tokyo) 14: 112—118

Geeves, M.A. & Holmes, K.C. (1999). Structural mechanism of muscle contraction. Annual Review of Biochemistry 68: 687—728

Fukushima, K. (1988). Application of the gas environmental chamber for electron microscopy. Ph.D Thesis (Nagoya University, Nagoya) (in Japanese)

Hibbard, M.G. & Trentham, D.R. (1986). Relationships between chemical and mechanical events during muscular contraction. Annual Review of Biochemistry 15: 119—161

Huxley, A.F. (1957). Muscle structure and theories of contraction. Progress in Biophysics and Biophysical Chemistry 7: 255—318

Huxley, A.F. (1998). Support for the lever arm. Nature 396: 317—318

Huxley, H.E. (1969). The mechanism of muscular contraction. Science 164: 1356—1366

Huxley, H.E. (1957). The double array of filaments in cross-striated muscle. Journal of Biophysical and Biochemical Cytology 3: 631—648

Huxley, H.E. & Hanson, J. (1954). Changes in the cross-striations of muscle during contraction and stretch and their structural interpretation. Nature 173: 973—976

Lymn, R.W. & Taylor, E.W. (1971). Mechanism of adenosine triphosphate hydrolysis by actomyosin. Biochemistry 10: 4617—4624

Margossian S.S. & Lowey, S. (1982). Hybridization and reconstruction of thick filament structure. Methods in Enzymology 85: 20—55

Minoda, H., Okabe, T., Inayoshi, Y., Miyakawa, T., Miyauchi, Y., Tanokura, S., Katayama, E., Wakabayashi, T., Akimoto, T. & Sugi, H. (2011). Electron microscopic evidence for the myosin head lever arm mechanism in hydrated myosin filaments using the gas

environmental chamber. Biochemical and Biophysical Research Communications. 405: 651—656

Oiw, K., Chaen, S. & Sugi, H. (1991). Measurement of work done by ATP-induced sliding between rabbit muscle myosin and algal cell actin cables in vitro. Journal of Physiology (London) 437: 751—763

Oiwa, K., Kawakami, T. & Sugi, H. (1993). Unitary distance of actin-myosin sliding studied using an in vitro force-movement assay system combined with ATP iontophoresis. Journal of Biochemistry (Tokyo) 114: 28—32

Page, S.G. & Huxley, H.E. (1963). Filament lengths in striated muscle. Journal of Cell Biology 19: 369—390

Perry, S.V. (1955). Myosin adenosine triphosphatase. Methods in Enzymology 2: 582—588

Suda, H., Ishikawa, A. & Fukami, A. (1992). Evaluation of the critical electron dose on the contractile activity of hydrated muscle fibers in the film-sealed environmental cell. Journal of Electron Microscopy 41: 223—229

Sugi, H. (1992). Molecular mechanism of actin-myosin interactionin muscle contraction. In: *Muscle contraction and Cell Motility*, Sugi,H (ed), Advances in Comparative & Environmental Physiology Vol.12, Springer, Berlin

Sugi, H., Akimoto, T., Sutoh, K., Chaen, S., Oishi, N. & Suzuki, S. (1997). Dynamic electron microscopy of ATP-induced myosin head movement in living muscle thick filaments. Proceedings of the National Academy of Sciences of the USA. 94: 4378—4382

Sutoh, K., Tokunaga, M. & Wakabayashi, T. (1989). Electron microscopic mapping of myosin head with site-directed antibodies. Journal of Molecular Biology 206: 357—363